Available online at www.sciencedirect.com
SCIENCE DIRECT
Tectonophysics 422 (2006) 159–173
TECTONOPHYSICS
www.elsevier.com/locate/tecto

Active transfer fault zone linking a segmented extensional system (Betics, southern Spain): Insight into heterogeneous extension driven by edge delamination

José Miguel Martínez-Martínez [a,*], Guillermo Booth-Rea [b], José Miguel Azañón [a], Federico Torcal [c]

[a] *Instituto Andaluz de Ciencias de la Tierra and Departamento de Geodinámica (C.S.I.C. — Universidad de Granada, Avenida Fuentenueva s/n, 18071 — Granada, Spain*
[b] *Departamento de Geodinámica, Universidad de Granada, Avenida Fuentenueva s/n, 18071 — Granada, Spain*
[c] *Departamento de Ciencias Ambientales, Facultad de Ciencias Experimentales, Universidad Pablo Olavide, 41013 — Sevilla, Spain*

Received 12 January 2006; received in revised form 6 June 2006; accepted 8 June 2006
Available online 18 July 2006

Abstract

Pliocene and Quaternary tectonic structures mainly consisting of segmented northwest–southeast normal faults, and associated seismicity in the central Betics do not agree with the transpressive tectonic nature of the Africa–Eurasia plate boundary in the Ibero-Maghrebian region. Active extensional deformation here is heterogeneous, individual segmented normal faults being linked by relay ramps and transfer faults, including oblique-slip and both dextral and sinistral strike-slip faults. Normal faults extend the hanging wall of an extensional detachment that is the active segment of a complex system of successive WSW-directed extensional detachments which have thinned the Betic upper crust since middle Miocene. Two areas, which are connected by an active 40-km long dextral strike-slip transfer fault zone, concentrate present-day extension. Both the seismicity distribution and focal mechanisms agree with the position and regime of the observed faults. The activity of the transfer zone during middle Miocene to present implies a mode of extension which must have remained substantially the same over the entire period. Thus, the mechanisms driving extension should still be operating. Both the westward migration of the extensional loci and the high asymmetry of the extensional systems can be related to edge delamination below the south Iberian margin coupled with roll-back under the Alborán Sea; involving the asymmetric westward inflow of asthenospheric material under the margins.

Keywords: Transfer faults; Extensional systems; Active tectonics; Earthquake focal mechanisms; Betics

1. Introduction

The Betics in southern Spain form part of the Ibero-Maghrebian region, which is characterized by active deformation and diffuse seismicity, associated with NW–SE Africa–Europe convergence (e.g. Argus et al., 1989; Kiratzi and Papazachos, 1995, Stich et al., 2003; Fernandes et al., 2004; Nocquet and Calais, 2004). Seismicity is distributed over a widespread area from the southern Iberian Peninsula to the High Atlas in Morocco, as would be expected in a continent–continent collision (Fig. 1). The diffuse pattern of regional seismicity does

* Corresponding author. Tel.: +34 958 249504; fax: +34 958 248527.
E-mail address: jmmm@ugr.es (J.M. Martínez-Martínez).

0040-1951/$ - see front matter © 2006 Elsevier B.V. All rights reserved.
doi:10.1016/j.tecto.2006.06.001

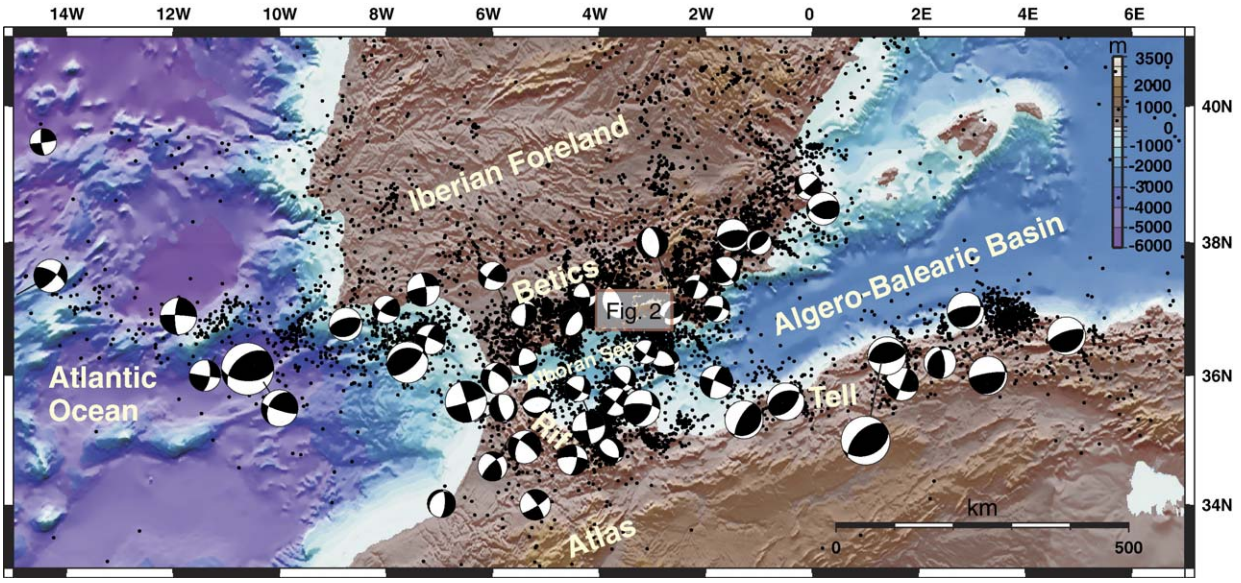

Fig. 1. Tectonic sketch of the Ibero-Maghrebian region including the seismicity distribution for the period 1973–2005 (USGS/NEIC data file). Focal mechanism solutions are collected from Grimison and Chen (1986), Medina and Cherkaoui (1992), Buforn et al. (2004) and Stich et al. (2003). Study area in square.

not allow delineating the present-day European–African plate boundary in this sector. Several seismotectonic studies carried out in order to characterize the dynamic behaviour of this area of continental deformation have revealed a complex seismotectonic pattern (e.g. Grimison and Chen, 1986; Buforn et al., 1995; Morel and Meghraoui, 1996; Stich et al., 2003; Buforn et al., 2004). Taking into account both active structures and focal mechanism solutions for earthquakes of small and moderate magnitude, the Ibero-Maghrebian region can be subdivided into five main active zones (Fig. 1): (1) the Tell–Atlas zone mainly showing NE–SW striking reverse faults with thrust fault focal mechanism solutions; (2) the eastern Betics–Alborán with predominant strike-slip fault mechanisms and both dextral NW–SE and sinistral N–S striking faults (e.g. Weijermars, 1987; Montenat and Ott d'Estevou, 1990; Booth-Rea et al., 2004b); (3) the Rif region with a complex seismotectonic pattern including focal mechanism solutions with WSW–ENE extension, NE–SW fault planes with dextral strike-slip mechanisms, and sinistral strike-slip mechanisms with E–W fault planes, among others (Morel and Meghraoui, 1996; Stich et al., 2003); (4) the central Betics also showing a complex seismotectonic pattern with predominant extensional deformation and a great variability of focal mechanisms (e.g. Galindo-Zaldívar et al., 1999; Muñoz et al., 2002; Stich et al., 2003); and (5) the Atlantic zone showing E–W striking fault planes with dextral strike-slip mechanisms and NE–SW thrusts (e.g. Morel and Meghraoui, 1996; Ribeiro et al., 1996).

A great part of this active deformation can be attributed to NW–SE convergence, even though active deformation in both Rif and central Betics does not fit in with this geodynamic scenario. Morel and Meghraoui (1996) suggested that the Gorringe–Alborán–Tell zone may be a 50–100-km wide transpression zone where active thrust faults would be controlled by deep-seated dextral transcurrent faults. This model avoids addressing the active deformation in the Betics and Alborán Sea. Models based on thin-shell finite elements emphasize also the transpressive nature of the Africa–Eurasia plate boundary (Negredo et al., 2002; Jiménez-Munt and Negredo, 2003). Negredo et al. (2002) predict an increase in the westward component of the velocity field from east to west, suggesting that the Alborán domain is presently escaping in a WNW direction with a velocity of 3 mm yr^{-1} relative to stable Europe. These authors predict local active extension in regions of the Alborán Sea and in the central Betics in agreement with geological and seismological observations (e.g. Galindo-Zaldívar et al., 1999; Azañón et al., 2004; Buforn et al., 2004). However, extensional slip rates calculated by the thin-shell finite element models (average 0.04 mm yr^{-1} and maximum 0.1 mm yr^{-1}) are practically an order of magnitude lower than those measured in the field (0.4 mm yr^{-1} (Sanz de Galdeano et al., 2003); 0.35 mm yr^{-1} (Reicherter et al., 2003); 0.4–0.8 mm yr^{-1} (Ruiz et al., 2003); 0.1–0.48 mm yr^{-1} (Martínez-Díaz and Hernández-Enrile, 2004). Active extension occurs also in the western Alborán basin and Gibraltar Straits as deduced

from subsidence analysis at Sites ODP 976 (Rodríguez Fernández et al., 1999) and DSDP 121 (Hanne et al., 2003), and focal mechanisms (Stich et al., 2003; Buforn et al., 2004).

Solely transpressive models can explain part of the westward migration of the arc, and local extension in the Alborán Sea and central Betics, under slower displacement rates than measured in the field, but they fail to explain other geophysical and geological observations in the Ibero-Maghrebian region. First, tomographic images of the Gibraltar arc region show a clear eastward dipping slab interpreted as either subducted oceanic lithosphere or delaminated sub-continental lithospheric mantle (Seber et al., 1996; Calvert et al., 2000; Gutscher et al., 2002; Faccenna et al., 2004). Second, the intermediate and deep seismicity in the region defines the slab beneath the western Alborán Sea at intermediate depths (40–150 km) and beneath the central Betics at deep depths (600 km) (e.g. Seber et al., 1996; Buforn et al., 2004). Third, the Neogene to Quaternary evolution of volcanism in the region shows both subduction- and intraplate-related magmatism that has been related with retreating oceanic lithosphere beneath the Alborán Sea coupled with edge delamination in the Betic–Rif margins (Duggen et al., 2004, 2005). Replacement of cold lithosphere by asthenospheric mantle can explain part of the upper Miocene to Quaternary uplift of the Betic–Rif margins and the associated Messinian salinity crisis in the Mediterranean (Duggen et al., 2003).

This paper discusses the significance of active extension in the Betics–Rif–Alborán realm with the aim to understand the lithospheric processes that occur in the region. For this we show the kinematics and segmentation mode of the main Quaternary faults in the central Betics, with particular attention to the presence and meaning of active transfer faults. These data, combined with the study of new focal mechanism solutions for small magnitude shallow earthquakes, will enable us to understand the significance of active extension in the Betics and Alborán Sea, setting these processes in the regional context. We argue that the complex pattern of deformation can be explained in a scenario of heterogeneous active extension driven by edge-delamination of sub-continental lithospheric mantle under the Betics and Rif coupled with westerly-offset slab roll-back under the Alborán Sea.

2. Tectonic setting

The Betics in the westernmost Mediterranean region form the northern branch of an arched orogen (Gibraltar arc) resulting from Miocene collision between the Alborán domain and the south-Iberian and Maghrebian paleomargins in the context of N–S to NW–SE Africa–Iberia convergence (Fig. 1). Continental collision occurred after subduction of the "Flysch Trough" basement formed by oceanic or very thin continental crust that was the locus of deep-water sedimentation during the Mesozoic and part of the Cenozoic (Durand-Delga et al., 2000). The trough was likely between the above-mentioned paleomargins, along the length of the Iberia–Africa transform boundary, and spanned a larger area than the present Alborán Sea. Miocene collision produced tectonic inversion of both continental margins, causing development of a fold-and-thrust belt with westwards vergence (Platt et al., 1995; Crespo-Blanc and Campos, 2001; Platt et al., 2003a) while the hinterland was simultaneously extended (e.g. García-Dueñas and Martínez-Martínez, 1988, Platt and Vissers, 1989; Galindo-Zaldívar et al., 1989). Extension occurred initially along NNW-directed low-angle normal faults followed by more substantial extension along WSW-directed extensional detachments (García-Dueñas et al., 1992; Crespo-Blanc, 1995; Martínez-Martínez and Azañón, 1997; Booth-Rea et al., 2004a, 2005). Extension was heterogeneous thus resulting in different extensional styles from upper crustal extension characterized by core complex structures in the Betics to extension affecting the whole crust that resulted in extreme crustal thinning and strong subsidence in the Alborán Sea (Comas et al., 1999).

The mechanisms driving extension in a contractional tectonics setting are still being debated. In this respect, the different hypotheses can be grouped in two main types: one proposing slab roll-back of an east-dipping subducting oceanic lithosphere (Royden, 1993; Lonergan and White, 1997; Gutscher et al., 2002; Faccenna et al., 2004); the other proposing detachment of subcontinental lithosphere, either by delamination (García-Dueñas et al., 1992, Seber et al., 1996; Calvert et al., 2000), or convective removal of the lithospheric mantle (Platt and Vissers, 1989; Platt et al., 2003b). These two hypotheses could be reconciled in a geodynamic model recently proposed in which westward slab roll-back of subducted oceanic lithosphere beneath the Alborán Sea is coupled with delamination of subcontinental lithospheric mantle beneath the southern Iberian and northwestern African continental margins (Duggen et al., 2005). The issue of whether or not extension has ceased in the system is also controversial, especially when determining if the internal forces driving extension continue to operate. Some authors suggest active extension ceased in the Betics and the Alborán basin during the

upper Miocene (Tortonian) although thermal subsidence continued subsequently in the Alborán basin (Comas et al., 1992; Watts et al., 1993; Chalouan et al., 1997; Comas et al., 1999). Both the distribution of seismicity and the focal mechanism solutions in the central Betics, however, reveal active extension in the upper crust (Morales et al., 1997; Galindo-Zaldívar et al., 1999; Muñoz et al., 2002; Stich et al., 2003; Buforn et al., 2004). N–S contraction was active since the upper Miocene, generating large-scale upright E–W folds and conjugate strike-slip faults (e.g. Platt et al., 1983; Weijermars et al., 1985; Weijermars, 1987; Montenat and Ott d'Estevou, 1990; Booth-Rea et al., 2004b). A geometric and kinematic model has been recently proposed (Martínez-Martínez et al., 2002) to explain the close relationship between extension and shortening, as well as the kinematics and timing of low-angle extensional faulting and upright folding. Folding accompanied tectonic denudation, developing elongated domes with fold hinges both parallel (N–S contraction) and perpendicular (active extensional rolling hinge) to the direction of extension.

3. Active faults in central Betics

Compressional upper Miocene to present-day structures, including large-scale open folds and both reverse and transcurrent faults are predominant in the eastern Betics (e.g. Montenat and Ott d'Estevou, 1990; Stapel et al., 1996; Huibregtse et al., 1998; Booth-Rea et al., 2004b) and in a great part of the Alborán Sea (Morel and Meghraoui, 1996; Comas et al., 1999; Gràcia et al., 2006), in agreement with the current tectonic setting of NW–SE plate convergence. However, Quaternary normal faults and a relatively high concentration of earthquake epicentres characterize two main, but physically separated, areas of active extension in central Betics (Fig. 2). In the first one, namely the Granada basin, high-angle, NW–SE striking normal faults are predominant, but E–W and NE–SW normal faults occur locally (Galindo-Zaldívar et al., 1999; Muñoz et al., 2002). Evidence for the activity of both E–W and NW–SE normal faults is well documented from seismicity and offset of Holocene sediments (e.g. Alfaro et al., 2001; Reicherter et al., 2003; Azañón et al., 2004). The NW–SE faults form a segmented system, the en-echelon faults being linked by relay ramps or transfer faults, including oblique-slip and both sinistral (e.g. locality A, Fig. 2) and dextral strike-slip faults (Fig. 2). All of these normal faults extend the hanging wall of an active extensional detachment defined by a planar distribution of seismic foci at 15 km beneath the Granada basin (Morales et al., 1997). This detachment is the active segment of a complex system of successive WSW-directed extensional detachments that have thinned the Betic upper crust since the middle Miocene. Inactive segments of the detachment system were subsequently folded and they are exhumed in the core of the Sierra Nevada elongated dome (Martínez-Martínez et al., 2002).

The second area of active extension is found southwest of the Sierra de Gádor range (Fig. 2) where N–S to NW–SE, high-angle, normal faults delimit two large-scale eastward-tilted blocks. Pliocene delta sediments and Pleistocene glacis and alluvial fans are tilted by some of these faults, which control Holocene fluvial sedimentation (Martínez-Díaz and Hernández-Enrile, 2004; Marín-Lechado et al., 2005). Within a general diffuse pattern, the seismicity is relatively concentrated in this region, occurring in a NW–SE trending zone that extends offshore (Stich and Morales, 2001). Several other seismicity clusters occur south of the transfer fault zone, in the Sierra de la Contraviesa, probably related to other active faults of the extensional system (Fig. 2).

Footwall rocks in the Sierra Nevada and Sierra de Gádor lie at elevations that are 2000 to 2500 m higher than hanging wall rocks, which is consistent with the proposed extensional model. The Sierra de Gádor relief is due to domino-like rotation of large upper crustal blocks that produces the eastwards tilting of the topographic surface raising the western side of the block to 2200 m while the eastern one stands at a lesser elevation (<500 m) (Martínez-Díaz and Hernández-Enrile, 2004; Martínez-Martínez et al., 2004). The Sierra Nevada relief has been associated with the formation of the Sierra Nevada elongated dome. Doming was caused by the interference of two orthogonal sets of Miocene–Pliocene, large-scale open folds (trending roughly E–W and N–S) that warp both WSW-directed extensional detachments and the footwall regional foliation. N–S folds were generated by a rolling hinge mechanism while E–W folds formed due to shortening perpendicular to the direction of extension (Martínez-Martínez et al., 2004).

The above-described two active extensional areas are physically separated 40 km in an E–W direction but they are kinematically coupled through a WSW–ENE subvertical dextral strike-slip fault zone. Kinematic indicators in the associated fault rocks, including sub-horizontal striations, brittle S–C structures, asymmetric porphyroclasts in the fault gouge and the attitude of the cataclastic foliation, clearly point to a dextral sense of shear (Sanz de Galdeano et al., 1985; Martínez-Martínez, 2006). The strike-slip fault zone exhibits most of the characteristics of transfer faults as defined by Gibbs (1984): (1) the fault zone parallels the extension direction, (2) there is an

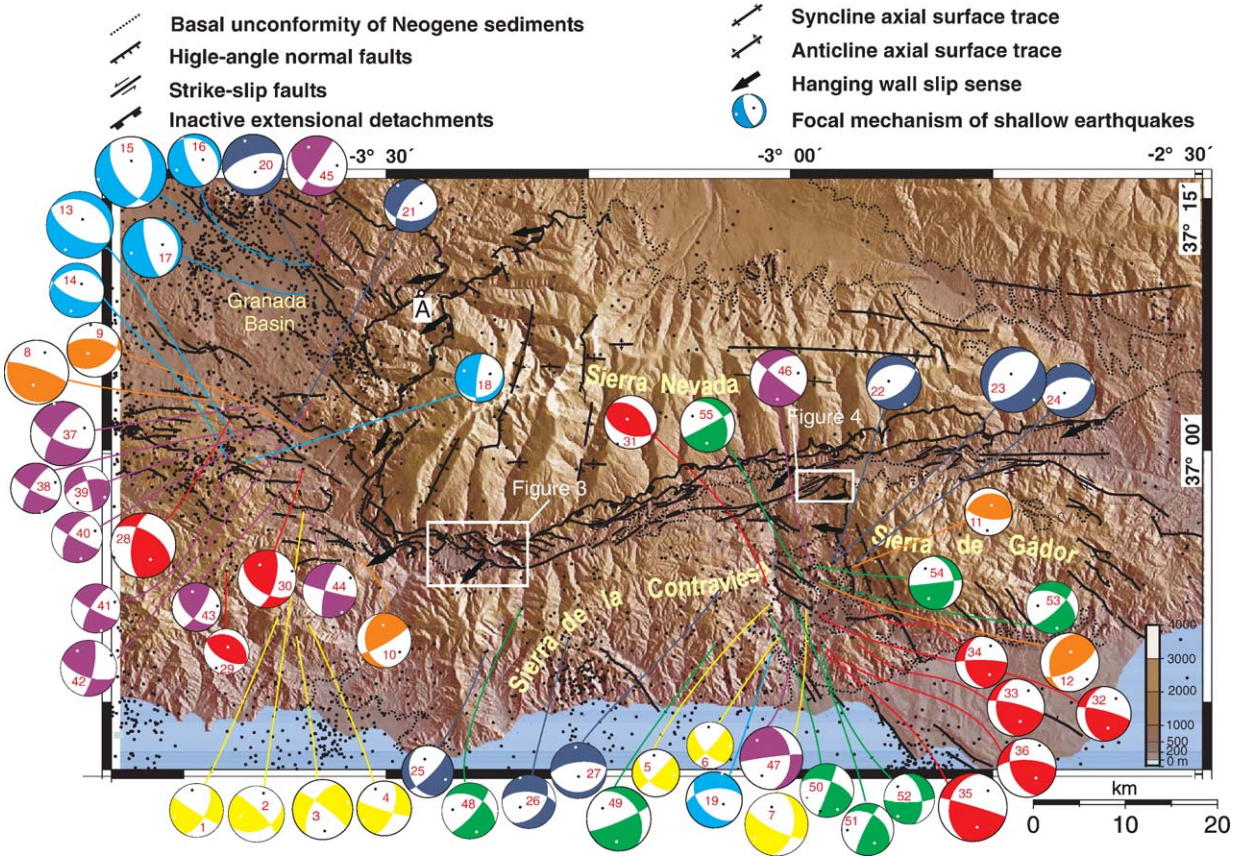

Fig. 2. Neotectonic and seismotectonic map of central Betics. Small black dots represent earthquake epicentres. Focal mechanism solution size is related to seismic magnitude ($2<m_b<3.8$). *P* and *T* axes are represented in black and white dots, respectively. Colours correspond to different types of focal mechanism solutions: Yellow, showing NW–SE striking fault planes with dextral strike-slip mechanisms and *P* axes trending around N–S. Orange, corresponding to reverse fault mechanisms with *P* axes trending N–S to NW–SE. Blue and dark blue corresponding to extensional fault mechanisms with NE–SW to E–W and N–S to NNW–SSE extension, respectively. Red, corresponding to reverse fault mechanisms with *P* axes trending NE–SW to E–W. Violet, corresponding to strike-slip fault mechanisms with *P* axes trending ENE–WSW and sinistral E–W to ESE–WNW fault planes. And green, corresponding to strike-slip fault mechanisms with *P* axes trending E–W to ESE–WNW and dextral NE–SW to E–W fault planes.

apparent lack of strike-slip offset along the fault or the offset is contrary to the slip, (3) detailed structural analysis of the strike-slip fault terminations demonstrates that the lower faults of the two active extensional areas coalesce with the strike-slip fault zone (Figs. 3 and 4). Both normal faults with NNE–SSW to N–S extension direction and reverse faults with WNW–ESE to W–E shortening direction occur near the strike-slip fault zone, compatible with the local strain field produced by an ENE orientated dextral shear couple. This fault zone is the southern boundary of a strike-slip related sedimentary basin with a middle Miocene to Quaternary infilling (Sanz de Galdeano et al., 1985; Martínez-Martínez, 2006). Deformation of Pliocene to Quaternary sediments along the fault zone provides evidence for recent fault activity (Figs. 5 and 6). Moreover, some fault segments laterally displace Quaternary alluvial fans and Holocene alluvial deposits (Figs. 3 and 4).

4. Focal mechanisms

Despite the diffuse nature of the seismicity, there are relative concentrations of epicentres showing NW–SE alignments in both areas of active extension (Fig. 2). Moreover, in the Granada basin epicentre alignments along E–W trending faults are also observed. Fault-plane solutions using P-wave first motion polarities have been determined for 68 earthquakes. We have selected the best 55 of them (see Plates 1, 2 and 3), which have been registered by at least 6 seismic stations; 27 in the Granada basin and surrounding areas and 28 in the tilted-block domain west of Sierra de Gádor (Fig. 2).

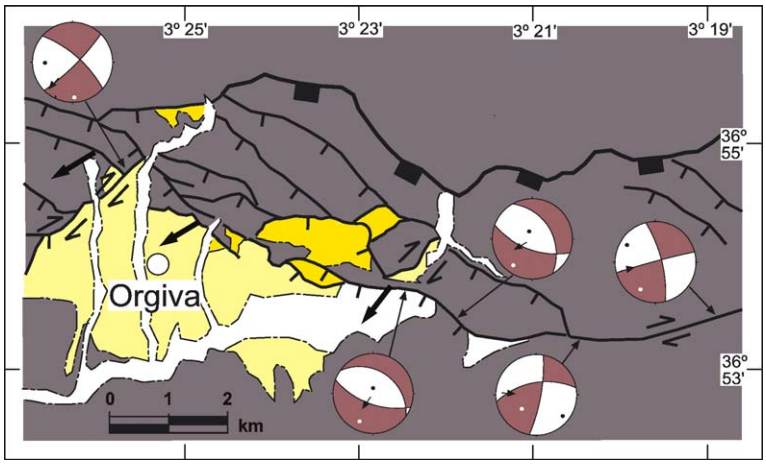

Fig. 3. Structural map of the Orgiva area showing the coalescence of both normal and strike-slip faults at the western end of the transfer fault zone. The main mapped faults and their striations are presented as focal mechanism solutions but the fault plane is known without ambiguity. Legend: Metamorphic basement in purple; Miocene sediments in yellow; Pliocene–Quaternary sediments in pale yellow; and Holocene sediments in white. Structure symbols as in Fig. 2. Location in Fig. 2.

Seismic magnitude is in general low ($2 < m_b < 3.8$) and the foci are confined to crustal depth of 3–19 km.

The focal mechanisms were calculated from earthquake data recorded between 1986 and 2002 (Table 1) by the Red Sísmica de Andalucía (RSA) of the Instituto Andaluz de Geofísica y Prevención de Desastres Sísmicos (IAGPDS) (Alguacil et al., 1990). The program Focmec (Snoke et al., 1984) included in SEISAN (Havskov and Ottemöller, 2001) was used to determine fault plane solutions using first motion polarities, considering all events were locatable in order to calculate angles of incidence. The solutions were constrained using only P-phase first motion polarities. The program makes a grid-search and finds how many polarities fit each possible solution. All solutions with less than a given number of wrong polarities are then written out and can be plotted. Calculations were performed considering a null maximum number of polarity errors, except for a few cases were 1 error was inevitable. The solutions were searched with a standard 5° increment,

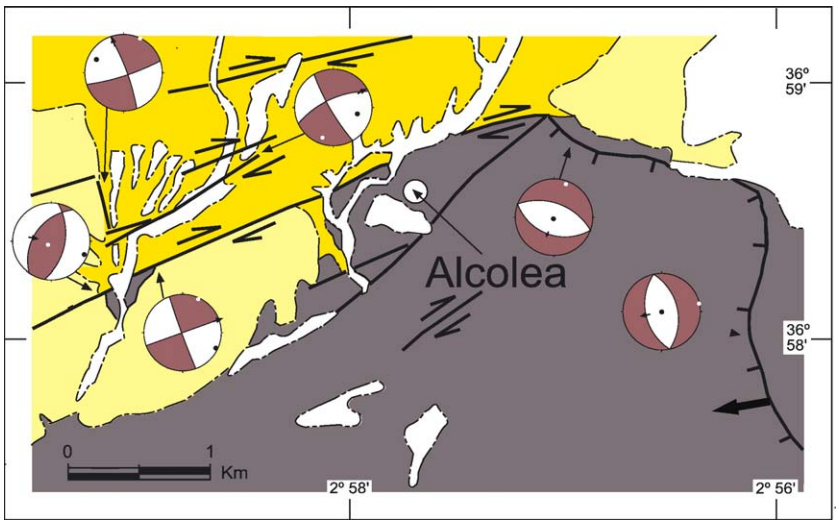

Fig. 4. Structural map of the Alcolea area showing the coalescence of both normal and strike-slip faults at the eastern end of the transfer fault zone. The main mapped faults and their striations are presented as focal mechanism solutions but the fault plane is known without ambiguity. The westernmost fault plane solution corresponds to a small-scale, not mapped fault. Legend as in Fig. 3. Structure symbols as in Fig. 2. Location in Fig. 2.

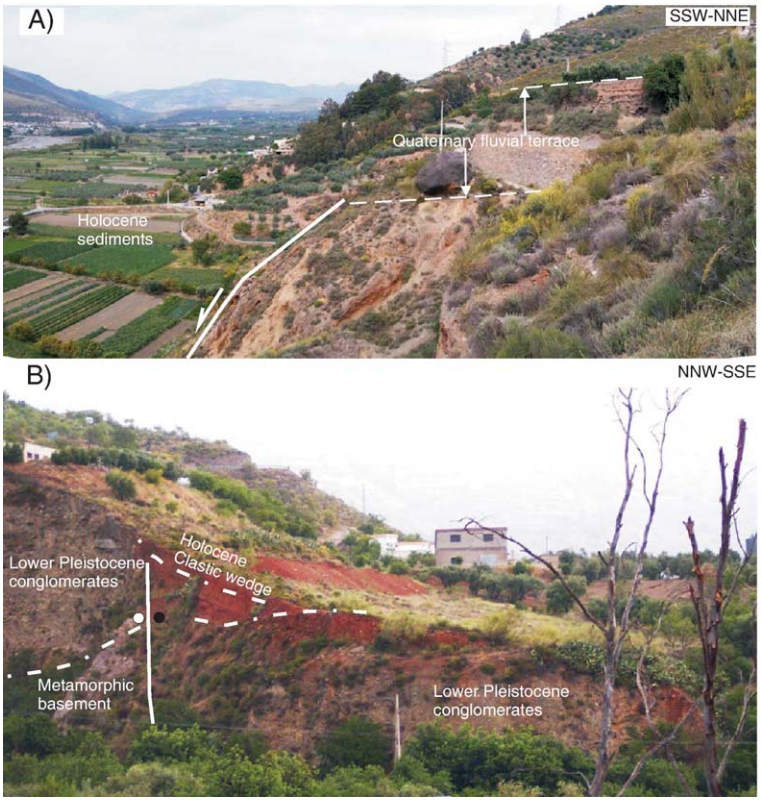

Fig. 5. Active structures in the western termination of the Alpujarras transfer fault zone. (A) Active frontal extensional ramp in the Orgiva basin. (B) Active dextral fault segment in the Orgiva basin.

however, in some cases extended to 10° when too many solutions were possible or reduced to 2° when only a few solutions were found possible.

All the earthquakes were located using the program HYP of SEISAN (Havskov and Ottemöller, 2001). The quality of the epicentre locations of the studied earthquakes is excellent or good, whilst the focal depth location quality is good or fair, depending on the seismic data available and the location of the seismic stations relative to the earthquake hypocentre. In the majority of the studied earthquakes the mean least squares error in the coordinates is between 0.1 and 0.4. Standard errors in latitude and longitude are between 1 and 7 km. The standard error in focal depth is normally below 4 km, although it is 9 km in two of the studied earthquakes.

Most focal mechanism solutions are incompatible with the regional stress field induced by NW–SE Africa–Iberia convergence. Only focal mechanism solutions 1–7 (Fig. 2), showing NW–SE striking fault planes with dextral strike-slip mechanisms, and focal mechanism solutions 8–12, showing roughly E–W reverse fault planes are compatible with the regional stress field. The remainder focal mechanism solutions show a great variability, suggesting a heterogeneous strain field for both areas of active extension. Within the shallow-depth range studied no correlation is observed between the different types of focal mechanisms and their hypocentral depth. Focal mechanism solutions 13 to 27 show extensional fault mechanisms with NE–SW to E–W (13–19) and N–S extension (29–27). Reverse fault mechanisms with *P* axis trending NW–SE to E–W are represented by focal mechanism solutions 28 to 36. The strike-slip mechanisms 37 to 55 exhibit *P*-axes varying around E–W directions. Focal mechanism solutions 37 to 47 with sinistral WNW–ESE fault planes mainly occur in the Granada basin, while focal mechanism solutions with dextral NE–SW to E–W fault planes (48 to 55) only appear in the Contraviesa region to the west of Sierra de Gádor (Fig. 2).

5. Discussion and conclusions

Focal mechanisms obtained in central Betics agree with others previously obtained both in the Granada basin (Muñoz et al., 2002) and in the western Sierra de Gádor area (Martínez-Díaz and Hernández-Enrile, 2004). The variability of focal mechanisms can be

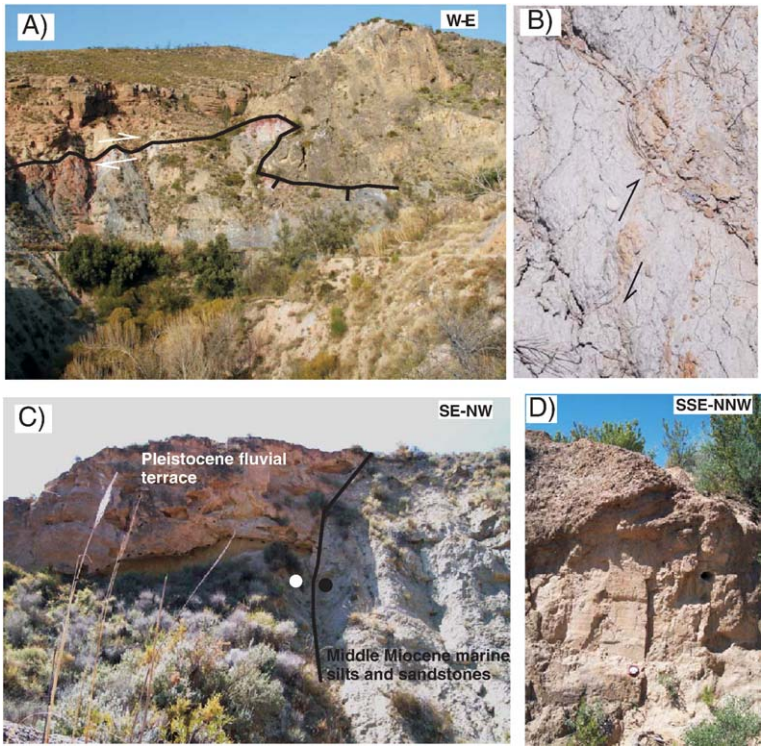

Fig. 6. Active fault segments in the eastern termination of the Alpujarras transfer fault zone. (A) Region where the transfer fault zone links with the Gádor frontal extensional ramp. (B) Rotated sandstone inclusion within marl fault gouge indicating vertical dextral shear in one of the transfer fault segments. The exposure is horizontal. The top right corner of the picture points to ENE. (C) Dextral transfer fault cutting a Pleistocene fluvial terrace. (D) Detail of striae associated with a sinistral fault cutting Pleistocene soils.

satisfactorily explained in the context of active, heterogeneous, WSW–ENE extension; where both dextral and sinistral WSW–ENE to E–W strike-slip faults occur (Figs. 2 and 7). The simultaneous activity of these strike-slip faults in the same region is incompatible with the transpressive regime of NW–SE Africa–Iberia convergence; however they fit well as transfer faults associated with the extensional system. Dextral transfer faults, generally striking parallel to the extension direction, induce local strain fields with axis of maximum shortening trending around NW–SE to E–W. In this local strain field both reverse fault mechanisms with *P* axis trending NW–SE to E–W and extensional fault mechanisms with N–S extension can occur. Moreover, the main mapped faults and their striations plotted as focal mechanisms reproduce most of the resolved focal mechanism solutions (Figs. 3 and 4).

Active extension has been documented in two separated areas of the central Betics, namely the Granada basin and the western Sierra de Gádor area, but no active relationship between the two extension loci has been suggested. Extension in the Granada basin has been attributed to collapse of the mountain front in a mainly compressive regime (Galindo-Zaldívar et al., 1999). However, Muñoz et al. (2002) interpret the Granada basin as a pull-apart basin bounded by two dextral WSW–ENE strike-slip faults compatible with the Africa–Iberia convergence. In contrast, Martínez-Martínez et al. (2002) suggest that active extension in this region is located in the upper plate of a detachment system whose active segment has migrated westward since the middle Miocene through a rolling hinge mechanism. Moreover, Martínez-Díaz and Hernández-Enrile (2004) consider extensional structures in the western Sierra de Gádor as related to local extension coupled with the present-day NNW–SSE compressional tectonics.

The linking of these two active extension zones by means of an extension related strike-slip fault (transfer fault) enhances the significance of active extension in the Betics and offers a new tectonic scenario for understanding the mechanisms driving extension in a continent–continent collisional tectonic setting. Transfer faults are an integral part of the extensional systems as seen in the oceanic transform faults; they form a useful reference frame parallel to the lineal velocity

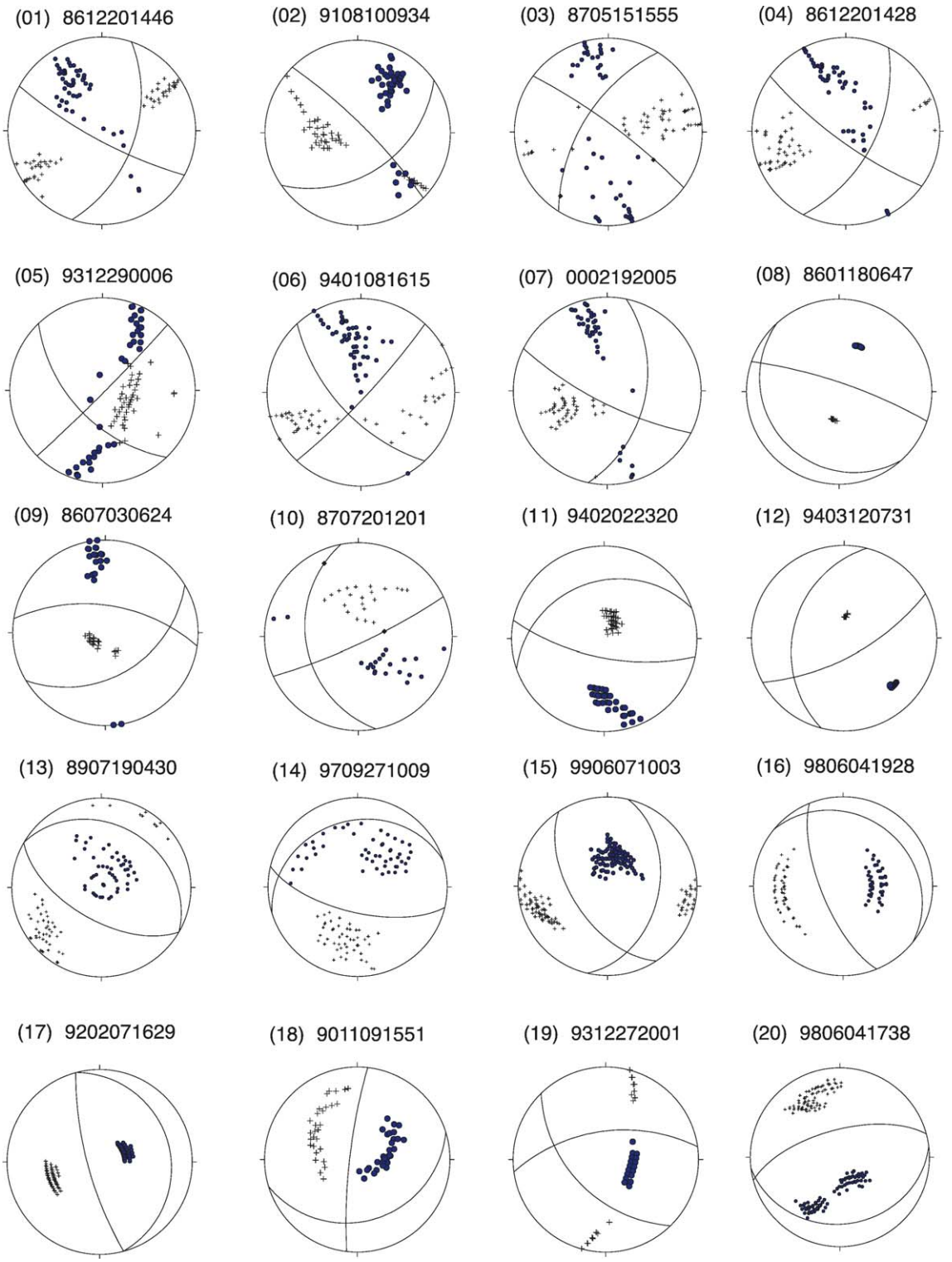

Plate I. Focal mechanisms of earthquakes studied in this paper obtained from polarities of P-waves. Event number, date and time are shown at the top. Crosses correspond to compressions and black dots to dilatations.

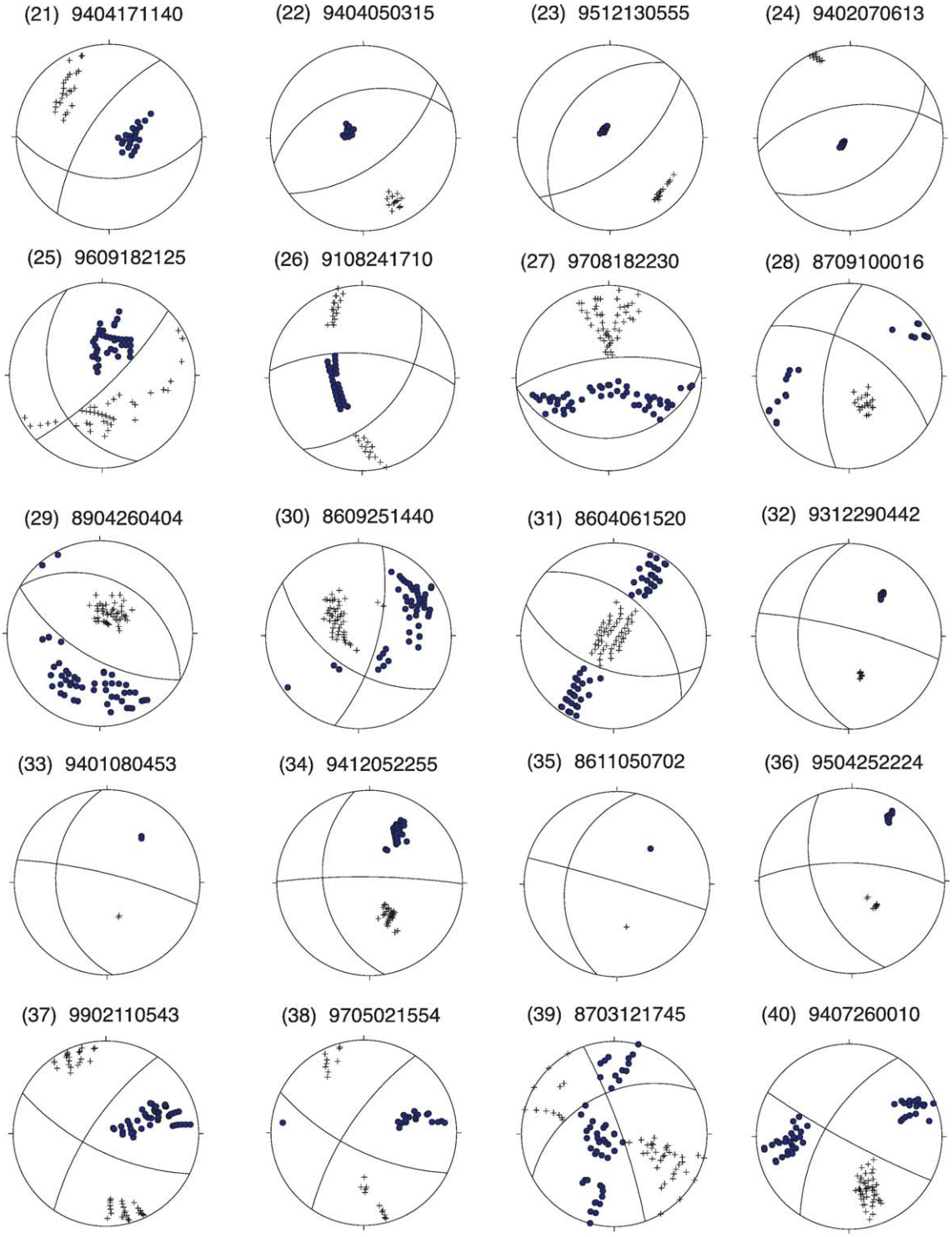

Plate II. Continuation of focal mechanisms of earthquakes studied in this paper obtained from polarities of P-waves. Event number, date and time are shown at the top. Crosses correspond to compressions and black dots to dilatations.

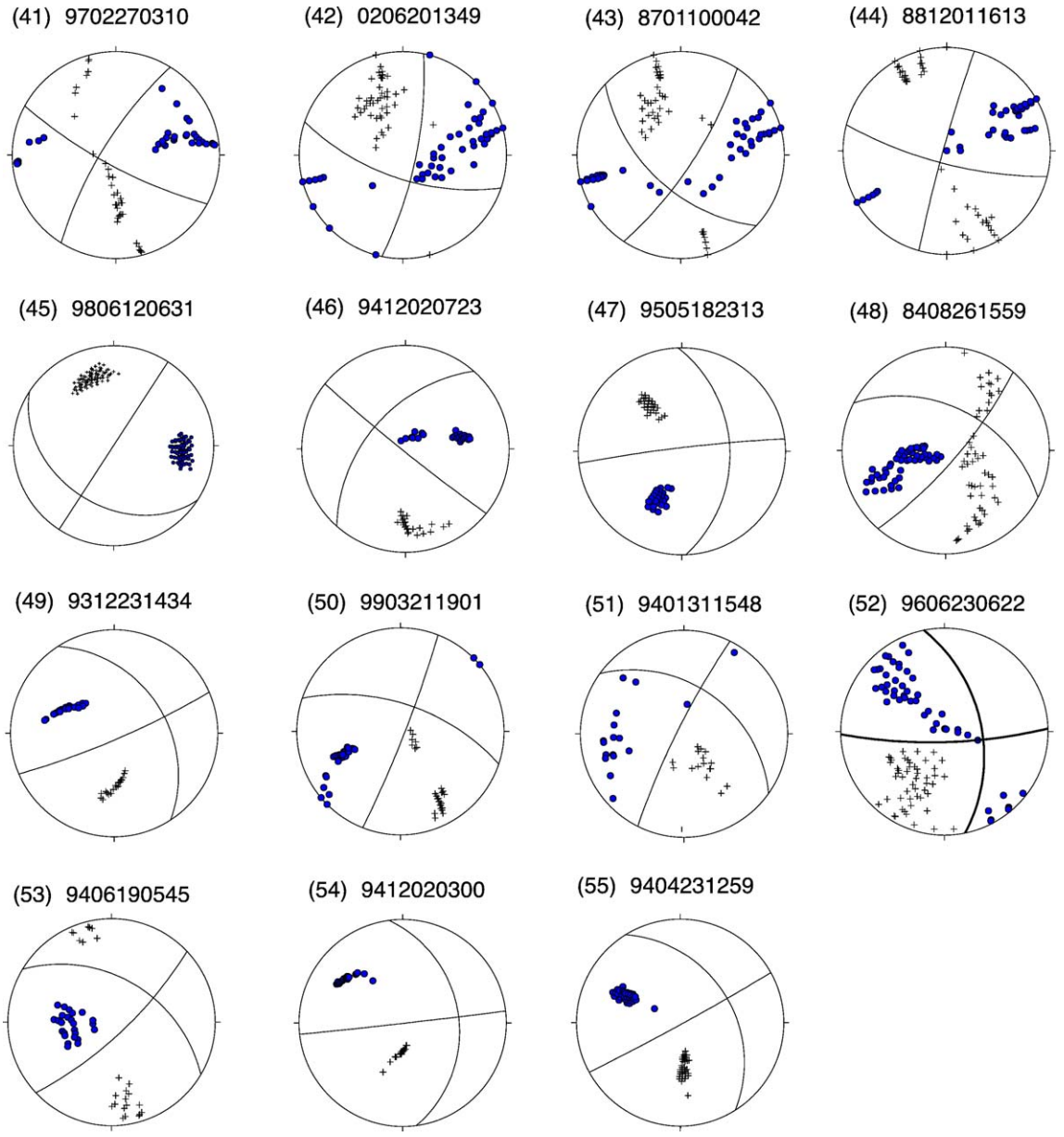

Plate III. Continuation of focal mechanisms of earthquakes studied in this paper obtained from polarities of P-waves. Event number, date and time are shown at the top. Crosses correspond to compressions and black dots to dilatations.

vectors. We have shown that some fault segments of the transfer zone are still active, at the same position since middle Miocene, thus involving a mode of extension that must have remained substantially the same over the entire period. From an actualistic point of view, the active extension represents a small increment in the extensional deformation history of the Betic hinterland. Areas showing active extension appear restricted in relation to the greater size of the extended domain, which implies important westward migration of the extension centres relative to the footwall as evidenced by apatite and zircon fission-track footwall ages (Johnson et al., 1997). Compressional structures east of the active extension centres suggest that the unloaded footwall was progressively shortened in N–S to NW–SE direction, when extension became inactive and, consequently, when forces related to the convergence were effective (Fig. 7). Lateral variations in the amount

Table 1
Source parameters of earthquakes analysed in this study

Event number	Event date	Origin time	Lat, deg	Long, deg	Number of stations	Z, km	Best fitting double couple (strike/dip/rake)	Magnitude m_b
01	861220	14:46:12.0	36.84	−3.64	7	9	122/84/−029, 028/61/−174	2.6
02	910810	09:34:51.4	36.95	−3.61	7	11	315/80/049, 055/42/165	2.8
03	870515	15:55:45.0	36.82	−3.61	8	8	307/81/−149, 212/59/−10	3.0
04	861220	14:28:28.6	36.83	−3.60	8	8	106/84/−29, 020/61/−173	2.6
05	931229	00:06:14.4	36.85	−3.03	6	9	045/87/−035, 136/54/−176	2.1
06	940108	16:15:44.7	36.82	−3.02	11	10	137/61/−009, 043/83/−151	2.1
07	000219	20.05:08.9	36.85	−2.98	14	5	117/75/−134, 012/45/−21	3.3
08	860118	06:47:48.5	37.05	−3.70	11	3	138/13/061, 289/79 /097	3.3
09	860703	06:24:32.3	37.01	−3.60	10	11	279/57/66, 059/40/123	2.6
10	870720	12:01:37.1	36.90	−3.54	9	7	060/81/060, 169/31/163	2.7
11	940202	23:20:43.2	36.89	−2.93	10	4	101/67/76, 251/27/116	2.1
12	940312	07:31:31.3	36.88	−2.97	11	7	195/32/129, 062/67/66	2.9
13	890719	04:30:49.4	37.02	−3.69	11	12	120/60/−090, 300/30/−090	3.6
14	970927	10:09:51.6	36.99	−3.70	8	16	253/27/−118, 103/67/−77	2.7
15	990607	10:03:12.8	37.22	−3.73	9	6	147/57/−118, 013/42/−053	3.8
16	980604	19:28:51.3	37.19	−3.60	8	10	158/70/−079, 309/22/−117	2.5
17	920207	16:29:13.5	37.16	−3.59	19	6	165/75/−090, 345/15/−090	3.0
18	901109	15:51:18.8	36.99	−3.68	8	13	187/81/−070, 073/22/−154	2.2
19	931227	20:01:58.6	36.81	−3.03	9	10	262/56/−053, 136/48/−132	2.8
20	980604	17:38:16.5	37.18	−3.60	8	10	070/25/−090, 253/65/−085	3.1
21	940417	11:40:40.2	37.03	−3.62	8	14	91/41/−041, 214/64/−123	2.5
22	940405	03:15:15.0	36.89	−2.95	15	4	254/36/−072, 053/56/−101	2.6
23	951213	05:55:32.5	36.90	−2.95	14	4	217/33/−079, 050/58/−097	3.4
24	940207	06:13:22.3	36.89	−2.92	15	5	262/51/−73, 054/42/−111	2.6
25	960918	21:25:14.9	36.81	−3.38	8	7	158/32/−153, 046/76/−060	2.4
26	910824	17:10:08.9	36.82	−3.28	9	5	039/45/−045, 274/60/−125	2.6
27	970818	22:30:07.9	36.87	−3.09	12	9	084/24/−090, 264/66/−090	2.8
28	870910	00:16:19.8	37.04	−3.70	18	5	302.6/54/144, 188/61/040	3.4
29	890426	04:04:24.2	36.88	−3.70	6	10	300/30/090, 120/60/090	2
30	860925	14:40:29.1	36.99	−3.61	8	13	015/66/043, 125/51/148	3
31	860406	15:20:39.1	36.87	−3.03	10	10	313/45/072, 109/49./106	2.5
32	931229	04:42:05.8	36.85	−2.98	8	10	284/81/122, 179/33/−017	2.6
33	940108	04:53:48.2	36.83	−2.95	14	10	284/80/121, 177/32/020	2.8
34	940125	22:55:10.5	36.85	−2.91	14	5	271/83/127, 171/37/013	2.4
35	861105	07:02:47.6	36.82	−2.97	11	17	286/88/122, 192/32/005	3.6
36	950425	22:24:21.7	36.81	−2.97	16	9	272/68/132, 159/46/031	2.9
37	990211	05:43:38.4	37.04	−3.67	9	18	214/71/−024, 116/67/−160	3.3
38	970502	15:54:36.5	37.03	−3.68	9	13	214/71/−024, 116/67/−160	2.5
39	870312	17:45:39.1	37.03	−3.64	7	12	242/43/−012, 341/82/−133	2.0
40	940726	00:10:28.9	37.00	−3.70	10	12	212/61/−007, 118/84/−151	2.4
41	970227	03:10:03.4	37.02	−3.67	9	12	212/75/−168, 118/77/−015	2.3
42	020620	13:49:53.1	37.01	−3.59	9	13	012/76/27, 289/64/163	2.8
43	870110	00:42:47.2	36.97	−3.62	6	15	033/75/037, 133/54./161	2.2
44	881201	16:13:52.9	36.95	−3.60	10	9	196/76/−004, 105/86/−165	2.7
45	980612	06:31:41.0	37.19	−3.59	6	10	123/40/0, 213/90/50	3.0
46	940122	07:23:35.3	36.89	−2.98	13	6	222/50/−177, 129/87/−040	2.8
47	950518	23:13:05.1	36.82	−3.00	16	10	358/40/−174, 263/86/−050	3.2
48	840826	15:59:10.2	36.85	−3.34	8	11	041/77/−046, 297/45/−161	2.8
49	931223	14:34:50.1	36.81	−3.09	18	19	327/37/−012, 067/83/−126	3.3
50	990321	19:01:01.5	36.84	−3.03	10	3	289/61/−006 , 021/85/−151	2.6
51	940131	15:48:15.8	36.82	−2.96	15	6	206/82/50, 305/41/168	2.5
52	960623	06:22:23.4	36.86	−3.00	9	9	348/51/−165, 088/78/−140	2.4
53	940619	05:45:58.4	36.88	−2.97	13	7	047/75/−048, 300/44/−158	2.5
54	940122	03:00:22.4	36.89	−2.98	11	6	352/33/−002, 084/89/−122	2.5
55	940423	12:59:04.3	36.88	−2.99	10	7	328/36/−004 , 061/88/−126	2.6

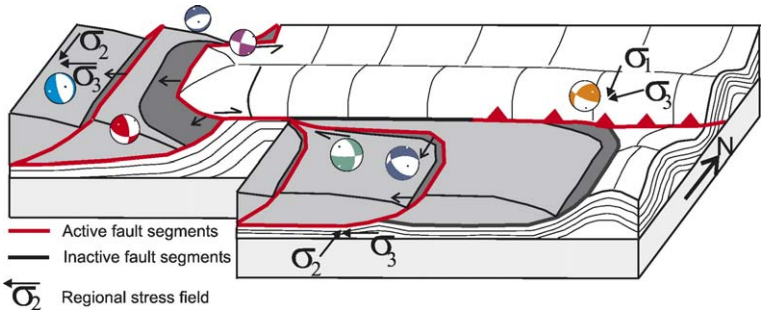

Fig. 7. Simplified model of the active kinematics of the Alpujarras transfer fault zone.

of shortening suggest that the contractional front migrated westward behind the loci of active extension (Martínez-Martínez et al., 2004).

On the basis of structural and sedimentary data from the eastern Betics and Alborán Sea, several authors consider that Miocene extension ceased at 9 Ma, a compressional stress field with a N–S to NW–SE shortening direction prevailing since then (Huibregtse et al., 1998, Comas et al., 1999). Cessation of extension has been attributed to a change in the direction of convergence, from N–S to NW–SE. Nevertheless, our extension model with westward migration of extensional loci and progressive shortening of the unloaded footwall contradicts such change in the tectonic regime. In our view, the change in the direction of convergence is not significant enough as to provoke a drastic change in the regional tectonic regime. We rather suggest that extension and shortening are and were coeval, but occurring at different loci and probably at different rates during the Neogene–Quaternary. Thus, the mechanisms driving extension since middle to upper Miocene should still be operating. Both the westward migration of the extensional loci and the high asymmetry of the extensional systems can be related to either a delamination mechanism (García-Dueñas et al., 1992, Seber et al., 1996; Calvert et al., 2000) involving the asymmetric westward inflow of asthenospheric material, to rollback of oceanic lithosphere (Royden, 1993; Lonergan and White, 1997; Gutscher et al., 2002) or most probably to a combination of both (Faccenna et al., 2004; Duggen et al., 2005).

The model above reconciles Neogene tectonics (e.g. Martínez-Martínez et al., 2002; Martínez-Martínez, 2006) and volcanism (e.g. Duggen et al., 2004) with a great body of recent data from the Ibero-Maghrebian region, including seismic tomography (Seber et al., 1996; Calvert et al., 2000; Gutscher et al., 2002; Faccenna et al., 2004), earthquake depth distribution (Seber et al., 1996; Buforn et al., 2004) and Quaternary to present tectonics in the Betics.

The formation of large ENE/WSW transfer fault zones could be favoured by a spatial offset between the delaminating lithosphere located under the active Granada basin and the retreating oceanic lithosphere front that occurs in a more westerly position, in the West Alborán basin and Gibraltar Straits, feature that can be observed in recent tomographic studies (Faccenna et al., 2004). Probably, other transfer faults exist, both dextral and sinistral. These faults are required to link the areas of active extension in the central Betics with those in the West Alborán basin, through the E–W-elongated depocentre of the Málaga graben in the north of the Alborán Sea (basins as denoted by Comas et al., 1999).

Acknowledgments

We thank A. Azor (Geodynamic Department of the Granada University) for constructive reading of the manuscript. Comments provided by E. Duebendorfer and an anonymous reviewer on an earlier version of the manuscript are also much appreciated and were very helpful in improving the paper. The research was supported by Comision Interministerial de Ciencia y Tecnología, Spain (CICYT) grants REN2001-3868-C03MAR, CGL2004-03333 and BTE2003-01699.

References

Alfaro, P., Galindo-Zaldívar, J., Jabaloy, A., López-Garrido, A.C., Sanz de Galdeano, C., 2001. Evidence for the activity and paleoseismicity of the Padul fault (Betic Cordillera, southern Spain). Acta Geol. Hisp. 36, 283–295.

Alguacil, G.A., Guirao, J.M., Gómez, F., Vidal, F., De Miguel, F., 1990. Red Sísmica de Andalucía (RSA): A digital PC-based seismic network, Seismic networks and rapid digital data transmission and exchange. Cahiers du Centre Européen de Géodynamique et de Séismologie, Walferdange, Luxembourg, pp. 19–27.

Argus, D.F., Gordon, R.G., DeMets, D., Stein, S., 1989. Closure of the Africa–Eurasia–North America plate motion circuit and tectonics of the Gloria fault. J. Geophys. Res. 94, 5585–5602.

Azañón, J.M., Azor, A., Booth-Rea, G., Torcal, F., 2004. Small-scale faulting, topographic steps and seismic risk in the Alhambra (Granada, SE Spain). J. Quat. Sci. 19 (3), 219–227.

Booth-Rea, G., Azañón, J.M., García-Dueñas, V., 2004a. Extensional tectonics in the northeastern Betics (SE Spain): case study of extension in a multilayered upper crust with contrasting rheologies. J. Struct. Geol. 26, 2039–2058.

Booth-Rea, G., Azañón, J.M., Azor, A., García-Dueñas, V., 2004b. Influence of strike-slip fault segmentation on drainage evolution and topography. A case study: the Palomares fault zone (southeastern Betics, Spain). J. Struct. Geol. 26, 1615–1632.

Booth-Rea, G., Azañón, J.M., Martínez-Martínez, J.M., Vidal, O., García-Dueñas, V., 2005. Contrasting structural and P–T evolutions of tectonic units in the southeastern Betics: key for understanding the exhumation of the Alborán domain HP/LT crustal rocks (Western Mediterranean). Tectonics 24. doi:10.1029/2004TC001640.

Buforn, E., Sanz de Galdeano, C., Udías, A., 1995. Seismotectonics of the Ibero-Maghrebian region. Tectonophysics 248, 247–261.

Buforn, E., Bezzeghoud, M., Udías, A., Pro, C., 2004. Seismic sources on the Iberia–African plate boundary and their tectonic implications. Pure Appl. Geophys. 161, 623–646.

Calvert, A., Sandvol, E., Seber, D., Barazangi, M., Roecker, S., Mourabit, T., Vidal, F., Alguacil, G., Jabour, N., 2000. Geodynamic evolution of the lithosphere and upper mantle beneath the Alborán region of the western Mediterranean: constraints from travel time tomography. J. Geophys. Res. 105, 10871–10898.

Chalouan, A., Rachida, S., Michard, A., Bally, A.W., 1997. Neogene tectonic evolution of the southwestern Alborán basin as inferred from seismic data of Morocco. AAPG Bull. 81, 1161–1184.

Comas, M.C., García-Dueñas, V., Jurado, M.J., 1992. Neogene tectonic evolution of the Alborán Sea from MCS data. Geo Mar. Lett. 12, 157–164.

Comas, M.C., Platt, J.P., Soto, J.I., Watts, A.B., 1999. The origin and tectonic history of the Alborán basin: Insights from Leg 161 Results. In: Zahn, R., Comas, M.C., Klaus, A. (Eds.), Proc. ODP Sci. Results, pp. 555–579.

Crespo-Blanc, A., 1995. Interference pattern of extensional fault systems: a case study of the Miocene rifting of the Alborán basement (North of Sierra Nevada, Betic chain). J. Struct. Geol. 17, 1559–1569.

Crespo-Blanc, A., Campos, J., 2001. Structure and kinematics of the South Iberian paleomargin and its relationship with the Flysch Trough units: extensional tectonics within the Gibraltar Arc fold-and-thrust belt (western Betics). J. Struct. Geol. 23, 1615–1630.

Duggen, S., Hoernle, K., van den Bogaard, P., Rupke, L., Phipps Morgan, J., 2003. Deep roots of the Messinian salinity crisis. Nature 422, 602–606.

Duggen, S., Hoernle, K., van den Bogaard, P., Harris, C., 2004. The role of subduction in forming the western Mediterranean and causing the Messinian salinity crisis. Earth Planet. Sci. Lett. 218, 91–108.

Duggen, S., Hoernle, K., Van den Bogaard, P., Garbe-Schonberg, D., 2005. Post-collisional transition from subduction- to intraplate-type magmatism in the westernmost Mediterranean: evidence for continental-edge delamination of subcontinental lithosphere. J. Petrol. 46, 1155–1201.

Durand-Delga, M., Rossi, P., Olivier, P., Puglisi, D., 2000. Situation structurale et nature ophiolitique des roches basiques jurassiques associées aux flyschs maghrébins du Rif (Maroc) et de Sicile (Italie). C. R. Acad. Sci. Paris 331, 29–38.

Faccenna, C., Piromallo, C., Crespo-Blanc, A., Jolivet, L., Rossetti, F., 2004. Lateral slab deformation and the origin of the western Mediterranean arcs. Tectonics 23. doi:10.1029/2002TC001488 (TC1012).

Fernandes, R.M.S., Ambrosius, B.A.C., Noomen, R., Bastos, L., Combrinck, L., Miranda, J.M., Spakman, W., 2004. Angular velocities of Nubia and Somalia from continuous GPS data: implications on present-day relative kinematics. Earth Planet. Sci. Lett. 222, 197–208.

Galindo-Zaldívar, J., González-Lodeiro, F., Jabaloy, A., 1989. Progressive extensional shear structures in a detachment contact in the Western Sierra Nevada (Betic Cordilleras, Spain). Geodin. Acta 3, 73–85.

Galindo-Zaldívar, J., Jabaloy, A., Serrano, I., Morales, J., González-Lodeiro, F., Torcal, F., 1999. Recent and present-day stresses in the Granada basin (Betic Cordilleras): example of a late Miocene–present-day extensional basin in a convergent plate boundary. Tectonics 18, 686–702.

García-Dueñas, V., Martínez-Martínez, J.M., 1988. Sobre el adelgazamiento mioceno del dominio cortical de Alborán, el despegue extensional de Filabres (Béticas orientales). Geogaceta 5, 53–55.

García-Dueñas, V., Balanyá, J.C., Martínez-Martínez, J.M., 1992. Miocene extensional detachments in the outcropping basement of the northern Alborán basin (Betics) and their tectonic implications. Geo Mar. Lett. 12, 88–95.

Gibbs, A.D., 1984. Structural evolution of extensional basin margins. J. Geol. Soc. (Lond.) 141, 609–620.

Gràcia, E., Pallàs, R., Soto, J.I., Comas, M.C., Moreno, X., Masana, E., Santanach, P., Diez, S., García, M., Dañobeitia, J., HITS scientific party, 2006. Active faulting offshore SE Spain (Alborán Sea): Implications for earthquake hazard assessment in the southern Iberian margin. Earth Planet. Sci. Lett. 241, 734–749.

Grimison, N.L., Chen, W., 1986. The Azores–Gibraltar plate boundary; focal mechanisms, depth of earthquakes and their tectonic implications. J. Geophys. Res. 91, 2029–2047.

Gutscher, M.A., Malod, J., Rehault, J.P., Contrucci, I., Klingelhoefer, F., Mendes-Victor, L., Spakman, W., 2002. Evidence for active subduction beneath Gibraltar. Geology 30, 1071–1074.

Hanne, D., White, N., Lonergan, L., 2003. Subsidence analyses from the Betic Cordillera, southeast Spain. Basin Res. 15, 1–21.

Havskov, J., Ottemöller, L., 2001. Seisan: The Earthquake Analysis Software, Version 7.2. Institute of Solid Earth Physics, University of Bergen, Norway.

Huibregtse, P., van Alebeek, H., Zall, M., Biermann, C., 1998. Paleostress analysis of the northern Nijar and southern Vera basins: constraints for the Neogene displacement history of major strike-slip faults in the Betic Cordilleras, SE Spain. Tectonophysics 300, 79–101.

Jiménez-Munt, I., Negredo, A.M., 2003. Neotectonic modelling of the western part of the Africa–Eurasia plate boundary: from the Mid-Atlantic ridge to Algeria. Earth Planet. Sci. Lett. 205, 257–271.

Johnson, C., Harbury, N., Hurford, A.J., 1997. The role of extension in the Miocene denudation of the Nevado–Filabride Complex, Betic Cordillera (SE Spain). Tectonics 16, 189–204.

Kiratzi, A.A., Papazachos, C.B., 1995. Active crustal deformation from the Azores triple junction to the Middle East. Tectonophysics 243, 1–24.

Lonergan, L., White, N., 1997. Origin of the Betic–Rif mountain belt. Tectonics 16, 504–522.

Marín-Lechado, C., Galindo-Zaldívar, J., Rodríguez-Fernández, L.R., Serrano, I., Pedrera, A., 2005. Active faults, seismicity and stresses in an internal boundary of a tectonic arc (Campo de Dalías and Níjar, southeastern Betic Cordilleras, Spain). Tectonophysics 396, 81–96.

Martínez-Díaz, J.J., Hernández-Enrile, J.L., 2004. Neotectonics and morphotectonics of the southern Almería region (Betic Cordillera–Spain) kinematic implications. Int. J. Earth Sci. 93, 189–206.

Martínez-Martínez, J.M., 2006. Lateral interaction between metamorphic core complexes and less-extended, tilt-block domains: the Alpujarras strike-slip transfer fault zone (Betics, SE Spain). J. Struct. Geol. 28, 602–620.

Martínez-Martínez, J.M., Azañón, J.M., 1997. Mode of extensional tectonics in the southeastern Betics (SE Spain). Implications for the tectonic evolution of the peri-Alborán orogenic system. Tectonics 16, 205–225.

Martínez-Martínez, J.M., Soto, J.I., Balanyá, J.C., 2002. Orthogonal folding of extensional detachments: structure and origin of the Sierra Nevada elongated dome (Betics, SE Spain). Tectonics 21. doi:10.1029/2001TC001283.

Martínez-Martínez, J.M., Soto, J.I., Balanyá, J.C., 2004. Elongated domes in extended orogens: a mode of mountain uplift in the Betics (Southeast Spain). In: Whitney, D.L., Teyssier, C., Siddoway, C.S. (Eds.), Gneiss Domes in Orogeny. GSA Special Paper, Boulder, Colorado, pp. 243–266.

Medina, F., Cherkaoui, T.E., 1992. Mécanismes au fayer des séismes du Maroc et des régions voisines (1956–1986). Conséquences tectoniques. Eclogae Geol. Helv. 85, 433–457.

Montenat, C., Ott d´Estevou, P., 1990. Eastern Betic Neogene basins— a review. In: Montenat, C. (Ed.), Les bassins Néogènes du Domaine Bétique Orientale (Espagne). Documents et Travaux IGAL, pp. 9–15.

Morales, J., Serrano, I., Vidal, F., Torcal, F., 1997. The depth of the earthquake activity in the central Betics (southern Spain). Geophys. Res. Lett. 24, 3289–3292.

Morel, J.L., Meghraoui, M., 1996. Goringe–Alborán–Tell tectonic zone: a transpression system along the Africa–Eurasia plate boundary. Geology 24, 755–758.

Muñoz, D., Cisternas, A., Udías, A., Mezcua, J., Sanz de Galdeano, C., Morales, J., Sánchez-Venero, M., Haessler, H., Ibáñez, J., Buforn, E., Pascal, G., Rivera, L., 2002. Microseismicity and tectonics in the Granada basin (Spain). Tectonophysics 356, 233–252.

Negredo, A.M., Bird, P., Sanz de Galdeano, C., Buforn, E., 2002. Neotectonic modeling of the Ibero-Maghrebian region. J. Geophys. Res. 107 (B11), 2292. doi:10.1029/2001JB000743.

Nocquet, J.-M., Calais, E., 2004. Geodetic measurements of crustal deformation in the western Mediterranean and Europe. Pure Appl. Geophys. 161, 661–681.

Platt, J.P., Vissers, R.L.M., 1989. Extensional collapse of thickened continental lithosphere: a working hypothesis for the Alborán Sea and Gibraltar arc. Geology 17, 540–543.

Platt, J.P., Van der Eeckhout, B., Janzen, E., Konert, G., Simon, O.J., Weijermars, R., 1983. The structure and tectonic evolution of the Aguilón fold-nappe, Sierra Alhamilla, Betic Cordilleras, SE Spain. J. Struct. Geol. 5, 519–535.

Platt, J., Allerton, S., Kirker, A., Platzman, E., 1995. Origin of the western Subbetic arc (south Spain) — paleomagnetic and structural evidence. J. Struct. Geol. 17, 765–775.

Platt, J.P., Allerton, S., Kirker, A., Mandeville, C., Mayfield, A., Platzman, E.S., Rimi, A., 2003a. The ultimate arc: differential displacement, oroclinal bending, and vertical axis rotation in the External Betic–Rif arc. Tectonics 22. doi:10.1029/2001TC001321.

Platt, J.P., Whitehouse, M.J., Kelley, S.P., Carter, A., Hollick, L., 2003b. Simultaneous extensional exhumation across the Alborán basin: implications for the causes of late orogenic extension. Geology 31, 251–254.

Reicherter, K.R., Jabaloy, A., Galindo-Zaldivar, J., Ruano, P., Becker-Heidmann, P., Morales, J., Reiss, S., González-Lodeiro, F., 2003. Repeated palaeoseismic activity of the Ventas de Zafarraya fault (S Spain) and its relation with the 1884 Andalusian earthquake. Int. J. Earth Sci. 92, 912–922.

Ribeiro, A., Cabral, J., Baptista, R., Matias, L., 1996. Stress pattern in Portugal mainland and the adjacent Atlantic region, West Iberia. Tectonics 15, 641–659.

Rodríguez Fernández, J., Comas, M.C., Soria, J., Martín Pérez, J.A., Soto, J.I., 1999. The sedimentary record of the Alborán basin: an attempt at sedimentary sequence correlation and subsidence analysis. In: Zahn, R., Comas, M.C., Klaus, A. (Eds.), Proc. ODP Sci. Results, pp. 69–76.

Royden, L.H., 1993. Evolution of retreating subduction boundaries formed during continental collision. Tectonics 12, 629–638.

Ruiz, A.M., Ferhat, G., Alfaro, P., Sanz de Galdeano, C., Lacy, M.C., Rodríguez-Caderot, G., Gil, A.J., 2003. Geodetic measurements of crustal deformation on NW–SE faults of the Betic Cordillera, southeastern Spain, 1999–2001. J. Geodyn. 35, 259–272.

Sanz de Galdeano, C., Rodriguez-Fernandez, J., López-Garrido, A.C., 1985. A strike-slip fault corridor within the Alpujarras mountains (Betic Cordilleras, Spain). Geol. Rundsch. 74, 641–655.

Sanz de Galdeano, C., Peláez Montilla, J.A., López Casado, C., 2003. Seismic potentiality of the main active faults in the Granada basin (south of Spain). Pure Appl. Geophys. 160, 1537–1556.

Seber, D., Barazangi, M., Ibenbrahim, A., Demnati, A., 1996. Geophysical evidence for lithospheric delamination beneath the Alborán Sea and Rif–Betic mountains. Nature 379, 785–790.

Snoke, J.A., Munsey, J.W., Teague, A.G., Bollinger, G.A., 1984. A program for focal mechanism determination by combined use of polarity and SV–P amplitude ratio data. Earthq. Notes 55, 15.

Stapel, G., Moeys, R., Biermann, C., 1996. Neogene evolution of the Sorbas basin (SE Spain) determined by paleostress analysis. Tectonophysics 255, 291–305.

Stich, D., Morales, J., 2001. The relative locations of multiplets in the vicinity of the western Almería (southern Spain) earthquake series of 1993–1994. Geophys. J. Int. 146, 801–812.

Stich, D., Ammon, C.J., Morales, J., 2003. Moment tensor solutions for small and moderate earthquakes in the Ibero-Maghreb region. J. Geophys. Res. 108. doi:10.1029/202JB002057.

Watts, A.B., Platt, J.P., Buhl, P., 1993. Tectonic evolution of the Alborán Sea basin. Basin Res. 5, 153–177.

Weijermars, R., 1987. The Palomares brittle–ductile shear zone of southern Spain. J. Struct. Geol. 9, 139–157.

Weijermars, R., Roep, T.B., Van den Eeckhout, B., Postma, G., Kleverlaan, K., 1985. Uplift history of a Betic fold nappe inferred from Neogene–Quaternary sedimentation and tectonics (in the Sierra Alhamilla and Almería, Sorbas and Tabernas basins of the Betic Cordilleras, SE Spain). Geol. Mijnb. 64, 397–411.